Biotechnology Reports 29 (2021) e00597

Contents lists available at ScienceDirect

Biotechnology Reports

journal homepage: www.elsevier.com/locate/btre

Research Article

# Characterizing the putative mitogen-activated protein kinase (*MAPK*) and their protective role in oxidative stress tolerance and carbon assimilation in wheat under terminal heat stress

Ranjeet R. Kumar[a,*], Kavita Dubey[a], Kirti Arora[a], Monika Dalal[b], Gyanendra K. Rai[c], Dwijesh Mishra[d], Krishna K. Chaturvedi[d], Anil Rai[d], Soora Naresh Kumar[e], Bhupinder Singh[e], Viswanathan Chinnusamy[f], Shelly Praveen[a,*]

[a] Division of Biochemistry, Indian Agricultural Research Institute, New Delhi, 110012, India
[b] ICAR-National Institute for Plant Biotechnology, Pusa Campus, New Delhi, 110012, India
[c] Sher-e-Kashmir University of Agricultural Sciences and Technology, Jammu, 180009, India
[d] CABin, Indian Agricultural Statistics Research Institute, New Delhi, 110012, India
[e] Centre for Environment Science and Climate Resilient Agriculture (CESCRA), Indian Agricultural Research Institute, New Delhi, 110012, India
[f] Division of Plant Physiology, Indian Agricultural Research Institute, New Delhi, 110012, India

ARTICLE INFO

*Article history:*
Received 15 December 2020
Received in revised form 28 January 2021
Accepted 3 February 2021

*Keywords:*
Mitogen-Activated protein kinases
Heat-Shock response
Recombinant fusion proteins
Triticum
Thermotolerance
Starch

ABSTRACT

Wheat, being sensitive to terminal heat, causes drastic reduction in grain quality and yield. MAPK cascade regulates the network of defense mechanism operated inside plant system. Here, we have identified 21 novel MAPKs through gel-based proteomics and RNA-seq data analysis. Based on digital gene expression, two transcripts (transcript_2834 and transcript_8242) showing homology with MAPK were cloned and characterized from wheat (acc. nos. MK854806 and KT835664). Transcript_2834 was cloned in pET28a vector and recombinant MAPK protein of ~40.3 kDa was isolated and characterized to have very high *in-vitro* kinase activity under HS. Native MAPK showed positive correlation with the expression of TFs, HSPs, genes linked with antioxidant enzyme (SOD, CAT, GPX), photosynthesis and starch biosynthesis pathways in wheat under HS. Wheat *cv.* HD3086 (thermotolerant) having higher expression and activity of MAPK under HS showed significant increase in accumulation of proline, $H_2O_2$, starch, and granule integrity, compared with BT-Schomburgk (thermosusceptible).



## 1. Introduction

Wheat is ancient and staple cereal crops grown in large part of the world under a wide range of agro-climatic regions. Major share of carbohydrate and calories in the diet are provided by wheat [1,2]. It contains 1.5–2% fat, 1.5–2% minerals, vitamins, and 2.2% crude fibers. Various abiotic stresses like drought stress, chilling injury, heat stress (HS), salinity stress, etc. have severe impact on the yield and grain-quality of wheat across the globe [3]. Terminal HS is defined as an elevation in temperature above ambient (>32 °C) during flowering and grain-filling stages [4,5]. Terminal HS has severe effect on different biological processes operating inside the plant system causing enormous losses in grain yield. Since, the ambient temperature is predicted to continue rising under climate change (1.5 °C between 2030 and 2052; IPCC, 2018), HS will be more severe for most of the agriculturally important crops, especially wheat [6]. The grain-quality and overall yield has been reported to be severely affected due to fluctuation in temperature during fertilization and grain-filling stages [7]. Heat stress during pollination stage causes formation of defunct pollen, unwinding of stigma, improper fertilization, false-seed setting, defragmentation of starch particles, and formation of shriveled grains [8]. Terminal HS reduces the grain-filling duration as well as the length of peduncle minimizing the total grain yield [1].

*Abbreviations:* HS, Heat stress; MAPK, Mitogen-activated protein kinase; 2-DE, 2-dimensional electrophoresis; SAGs, Stress-associated genes; SAPs, Stress-associated proteins; CD, Conserved domain; CAT, Catalase; HSR, Heat shock response; DGE, Digital gene expression.

* Corresponding authors.
*E-mail addresses:* ranjeet_biochem@iari.res.in (R.R. Kumar), dubeykavita786@gmail.com (K. Dubey), chugh.kirti29@gmail.com (K. Arora), monika@nrcpb.org (M. Dalal), gkrai75@gmail.com (G.K. Rai), dwij.mishra@gmail.com (D. Mishra), kkchaturvedi@gmail.com (K.K. Chaturvedi), Anil.Rai@icar.gov.in (A. Rai), nareshkumar.soora@gmail.com (S.N. Kumar), bhupindersinghiari@yahoo.com (B. Singh), viswa.chinnusamy@gmail.com, Viswanathan@iari.res.in (V. Chinnusamy), shellypraveen@hotmail.com (S. Praveen).

https://doi.org/10.1016/j.btre.2021.e00597

Wheat has inherent defence mechanism to protect itself from heat stress. Wide-diversity across the wheat genotypes has been observed for HS-tolerance. The inherent potential to sense the HS and trigger the defence mechanism, however, varies with the genotypes [9]. The signaling of plants under stress is basically a complexed network of interacting proteins working in cohesion in order to regulate the activation of the enzymes [3]. Signal transduction pathways in plants are very complex having significant cross-talks under different environmental cues [7,9]. MAPK is one of the most important signaling cascades operating inside the plant system and regulating the abiotic stress response of plants. Several cellular responses are linked with the external stimuli through MAPK cascade [10].

The MAPK cascade consists of MAPK kinase kinases (MAPKKKs), MAPK kinases (MAPKKs) and MAPK [11]. These are basically serine/threonine kinases (STKs) playing very important role in the regulation of key transcription factors (TFs) and pathway linked enzymes through phosphorylation/ dephosphorylation. MAPK signaling cascade has been reported to be triggered by several abiotic stresses in plant system [12]. MAPK genes has been mostly characterized in Arabidopsis, for example - *AtMPK3*, *AtMPK6*, *AtMPK1*, *AtMPK4*, *MAPKK*, and *MKK2* [13]. Genome mining of *Arabidopsis thaliana* showed the presence of ~110 genes linked with MAPK cascade kinases - 20 genes encodes for MAPK, 10 encodes for MAPKK, and 80 encodes for MAPKKK [14]. Similarly, genes involved in MAPK cascade has been reported and characterized in other closely related species, like rice, wheat, maize, etc. Genome mapping of rice showed the presence of 75, 8 and 17 MAPKKKs, MAPKKs, and MAPKs genes [15]. MAPK cascade also regulate ABA biosynthesis and in phosphorylation of various TFs like WRKY, HSF, etc. [16,17]. The complex genome of wheat was also scanned for the presence of *MAPK* and recently, 54 MAPK genes were identified [16]. MAPK cascade has not been much characterized in wheat especially for abiotic stress tolerance. MAPK cascade works as master switch (signaling/sensory protein molecule) in regulating the stresses by triggering the TFs and stress-associated genes [18]. However, very limited information on role of MAPK in thermotolerance of wheat is available on public domain.

## 2. Material and methods

### 2.1. Wheat genotypes and heat stress treatment

Wheat *cvs*. HD3086 (thermotolerant) and BT-Schomburgk (thermosusceptible) were selected for the present investigation. The seeds of both the *cvs*. were pre-treated with Bavistin @ 0.25% before sowing in 30 pots (15 pots per cultivar) having equal ratio of perlite, sand and farmyard manure (FYM). Pots were kept inside glass house with regulated growth conditions [22 ± 2 °C (day-time) and 18 ± 2 °C (night-time), RH of 80%, PAR of 250 μmol $m^{-1}$ $s^{-1}$ with 8 h light and dark period] at Mini Phytotron Facility, IARI, New Delhi. The plants were irrigated at regular interval. The plants (in group) were treated with differential HS ($T_1$ - 32°C, 2 h and $T_2$ - 38°C for 2 h) at flowering and grain development stages, decided based on the Feekes scale [19]. Microprocessor-regulated chambers were used to expose the plants to HS with an increment of 1 °C per 10 min, till it attains the specific temperature for HS. We have collected flag leaf and spikes in triplicates for further downstream applications.

### 2.2. Two-Dimensional polyacrylamide gel electrophoresis (2D-PAGE) for the identification of DEPs

The leaf samples collected from control (C - 22 ± 2 °C) and HS-treated ($T_2$ - 38 °C, 2 h) wheat *cvs*. were used for the 2-DE in order to identify the DEPs. 2D-Xtract kit (G Bioscience, USA) was used for the extraction and purification of total protein from 0.5 g tissue as per the instructions of the manufacturer. Other steps for the Isoelectric focusing (Ist dimension run) and Sodium dodecyl sulphate-polyacrylamide gel electrophoresis (IInd dimension run) were followed as mentioned in our earlier publication [20]. The 2-D Quant Kit (Amersham Biosciences, UK) was used for the protein quantitation. The IPG strips (18 cm, 3–10 linear pH gradients) was hydrated with 40 μg extracted protein diluted with rehydration buffer and IEF100 instrument was used for the separation of the proteins based on pI value. The image of the protein spots on the gels were scanned using Gel Documentation system (Bio-Rad, USA) and further, IMP7 version 7.0.6 software (GE Healthcare) was used for the image characterization. Based on the relative fold expression, 20 DEP spots (10 each) from HD3086 and BT-Schomburgk were used for the protein identification through MALDI-TOF/TOF MS analysis. The silver stained spots were picked up and processed for MALDI-TOF/TOF MS analysis as mentioned in Kumar et al. [21] and Kundu et al. [22].

### 2.3. Data mining for the identification of MAPK transcripts

The RNA-seq data generated earlier for the identification of SAGs in wheat under HS (https://www.ncbi.nlm.nih.gov/bioproject: PRJNA171754) was used for the identification of novel MAPK genes in wheat. We identified 21 putative transcripts showing homology with MAPK reported from different plants (Table S1). Even, the identified DEPs (as mentioned earlier) were characterized for their fold expression by calculating the ratio of pixilation of the protein spot in HS-treated upon the control. MAPK, being prominent DEPs, were further targeted for the identification of specific MAPK gene using reverse genetics approach.

### 2.4. Cloning of identified MAPK transcripts

For the cloning of identified transcripts, total RNA was isolated using the Trizol reagent (Invitrogen, UK). The qualitative assessment of total RNA was carried out using visualization on non-denaturating agarose gel electrophoresis followed by reading of Nanodrop (Thermo Scientific, U.S.A.). Total RNA having A260/A280 ratio of >1.9 was subsequently used for the cDNA synthesis using the Revert$^{Aid}$ H Minus First Strand cDNA Synthesis Kit (Thermo Scientific$^{TM}$, USA) following the manufacturers instruction.

Mining of transcriptome data showed the presence of 21 novel MAPK genes. The identified transcripts were mapped on the *Triticum aestivum* genome sequence available on Ensemble Plants (https://plants.ensembl.org/) for predicting the full length gene sequence. The predicted sequences were used for designing the forward and reverse oligo's using Genefisher2 primer designing software (Table S2). Reverse Transcriptase PCR (RT-PCR) and cloning were performed as mentioned in Kumar et al. [21]. Sanger's Di-deoxy method was used for the sequencing and further, the sequence of the genes were submitted in NCBI GenBank.

### 2.5. In-silico analysis of MAPK genes

The sequenced genes were used for the identification of closely related homologs using BLASTn and BLASTp tool of NCBI [23]. ORF finder was used for the prediction of open reading frame of the cloned genes (http://www.ncbi.nlm.nih). The amino acid sequences of the genes were predicted using Expasy tool (http://www.expasy.org/). The functional conserved domain was predicted using the CD search tool of NCBI (http://www.ncbi.nlm.nih.gov/Structure/cdd). NetPhosK was used for analyzing the kinase-specific phosphorylation sites (http://www.cbs.dtu.dk/services/NetPhosK/). The localization of the MAPK proteins was predicted

by identifying the signal peptide using Plant-PLOC (http://www.csbio.sjtu.edu.cn/bioinf/plant/). MAPKs reported from different plant and non-plant sources available on NCBI database were retrieved and further used for the clustalW alignment followed by phylogeny analysis using the NCBI tool.

### 2.6. Expression analysis using quantitative RT-PCR

Total RNA isolation and cDNA synthesis were performed as explained in above section. We have used diluted cDNA (100 ng $\mu L^{-1}$) for qRT-PCR reactions. Oligo's for the qRT-PCR was designed using Genefisher2 software. We selected heat-responsive transcription factors - *HSFA6e* (acc. no. KU291394.1), *WRKY* (acc. no. KU562861.1), HSPs - *HSP17* (acc. no. JN572711.1), *HSP26* (acc. no. AF097659.1)], antioxidant enzymes – *SOD* (acc. no. AF092524.1), *POX* (acc. no. AF005087.1) and starch biosynthesis pathway linked genes – ADP-glucose pyrophosphorylase (large subunit; acc. no. KC347594.1), soluble starch synthase gene (acc. no. KJ854903.1) for the expression analysis (Table S3). The samples were used in triplicates for the expression analysis. The expression was performed following the protocol as mentioned in Kumar et al. [20]. We have used β-actin gene (acc. no. AB181991.1) for normalizing the $C_t$ value. Further, Pfaffl method [24] was used for calculating the relative fold expression of the genes.

## 3. Heterologous expression of candidate MAPK gene

### 3.1. Primer designing, amplification and transformation

For the heterologous expression of the candidate MAPK gene, we designed gene-specific forward and reverse primers with restriction site of *Hin*dIII at 5′ end and *Xho*I at 3′ end using Genefisher2 software (Table S2). Oligo Analyzer (Integrated DNA Technologies, USA) was used for analyzing the quality of the oligo's. An amplicon of 1100 bp (coding region) containing *Hin*dIII and *Xho*I restriction sites were amplified using HiFi *Pfu* polymerase (Thermo Scientific, USA). The amplicon was double digested with *Hin*dIII and *Xho*I and again gel purified to be used for the ligation. The expression vector (*pET28a*) was linearized by double digestion with *Hin*dIII and *Xho*I followed by gel purification. The gel eluted MAPK gene was ligated with the linearized vector by incubating it at 16 °C for 16 h. The recombinant *pET28a*_MAPK plasmid was mobilized into *BL-21 (DE3)* strain of *E.coli.* Colony PCR and RE analysis was used for analyzing the positive transformants and other steps for

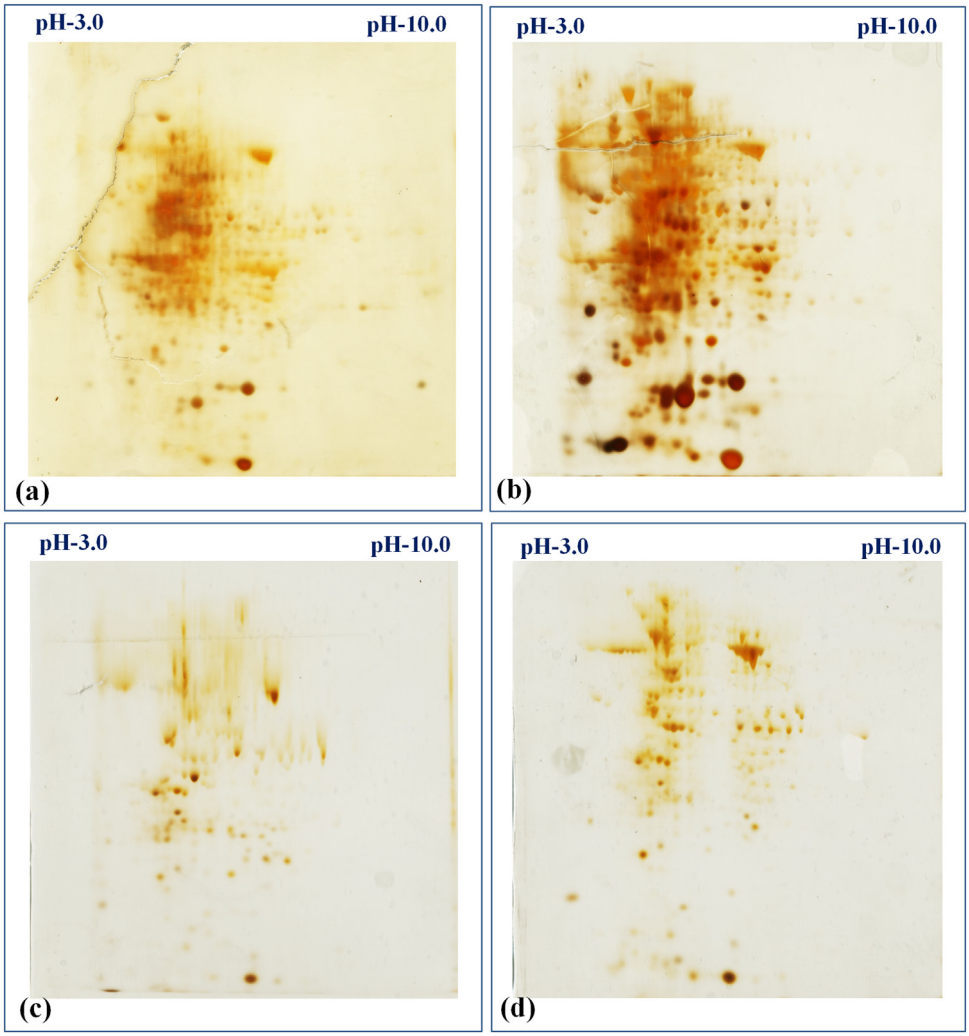


**Fig. 1.** Two dimensional polyacrylamide gel electrophoresis (2D-PAGE) for the identification of MAPK in wheat under HS, (a) expression of protein in HD3086 (thermotolerant) under control condition, (b) expression of proteins in HD3086 under HS-treated condition, (c) expression of protein in BT-Schomburgk (thermosusceptible) under control condition, (b) expression of proteins in BT-Schomburgk under HS-treated condition; C - 22 ± 3°C, HS - 38°C, 2 h; IPG strips in pH range of 3.0 to 10.0 was used for the isoelectric focussing (IEF).

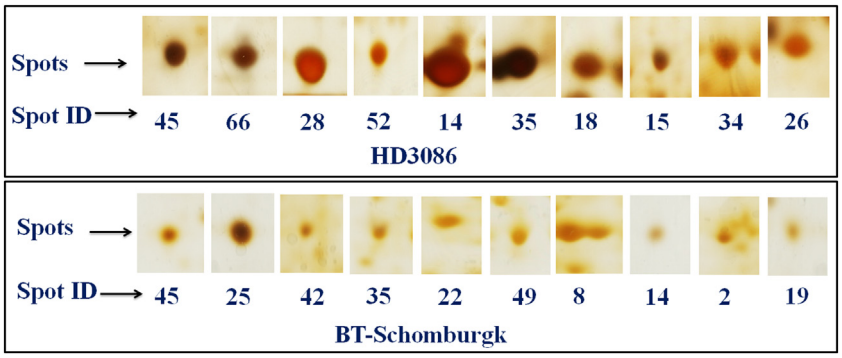


**Fig. 2.** Differentially expressed protein (DEPs) spots used for the identification using MALDI-TOF/ TOF-MS; Twenty spots were selected (10 each from both the *cvs.*) based on the relative fold expression.

the standardization of IPTG concentration, induction and purification of recombinant protein were followed as explained in Kumar et al. [21]. SDS-PAGE of induced (0.9 mM IPTG) and un-induced *E. coli* cells harboring the *pET28a*_MAPK was carried out on 12% resolving gel. The homogeneity and purity of the recombinant protein was analyzed by resolving it on the SDS-PAGE [25].

### 3.2. In vivo *and in vitro assay of MAPK protein*

The control and HS-treated leaves were used for the extraction, purification and activity assay of MAPK using ADP-Glo$^{TM}$ Kinase assay kit (Promega, USA). In brief, sample was extracted in 40 mM Tris (pH 7.5) and further, 20 mM $MgCl_2$, and 0.1 mg/mL BSA was added in the reaction mixture. The un-consumed ATP in the reaction mixture was depleted by adding 5 μL of ADP-Glo$^{TM}$reagent leaving only ADP. The RM was incubated at 25°C for 40 min. followed by addition of 10 μL of Kinase Detection Reagent in order to convert ADP to ATP. The ATP was quantified using the luciferase - luciferin system. A standard curve was prepared based on the comparison between% ATP to ADP conversion and relative light unit (RLU). The kinase assay was calculated as μmol/min/ mg of proteins. The activity assay of recombinant MAPK protein was carried out by using diluted protein (1:50) and other steps were followed as mentioned above. The recombinant protein was exposed to HS (C - 22 ± 3°C, $T_1$ - 32°C, 2 h, $T_2$ - 38°C, 2 h). We also used denatured (DN) recombinant MAPK protein as negative control. Total soluble protein was estimated using the Bradford method [26].

## 4. Estimation of thermotolerance linked biochemical markers

### 4.1. Activity assay of superoxide dismutase (SOD) enzyme

We have used the protocol of Beauchamp and Fridovich [27] for the SOD activity assay. The absorbance was taken at 560 nm against the reagent blank (phosphate buffer) and was further used for the calculation. The formula used was - SOD measured = [Control-(Sample-Blank)]/ Control *100; 50% inhibition in O.D. was considered as 1 unit of SOD activity.

### 4.2. Activity assay of catalase enzyme

Catalase enzyme was assayed in the samples following the protocol of Chance and Maehly [28]. In brief, crude extract was prepared from fresh leaf (1 g) homogenized in 5 mL of 50 mM $K_2HPO_4$ buffer (pH 7.0) along with 2 mM sodium-EDTA and 1% (w/v) PVP. A reaction mixture of 3 mL containing 2 mL of 100 mM $Na_2HPO_4$ buffer (pH 6.8), 0.5 mL of $H_2O_2$ (30 mM) and 0.5 mL enzyme was prepared and decline in the OD reading was read at 240 nm. Bradford method was used for the total soluble protein estimation [26].

### 4.3. Accumulation pattern of osmolyte

The proline content was estimated in the leaves following the protocol of Bates et al. [29]. We have used 0.1 g of leaf samples (0.1 g) for the crude extract preparation in 2.5 mL of 3% sulphosalicylic acid and other steps were followed as mentioned in the protocol.

### 4.4. Estimation of hydrogen peroxide ($H_2O_2$) accumulation in the cells

The protocol of Loreto and Velikova [30] was used for the estimation of $H_2O_2$ in the collected samples. Leaf samples (0.1 gm) were crushed in liquid $N_2$ and further homogenized in 1 mL of 1% Trichloroacetic acid. Further, reaction mixture was prepared by adding 0.75 mL of supernatant, 0.75 mL of phosphate buffer (10 mM, pH 7.0) and 1.5 mL of potassium iodide (KI) and the absorbance was taken at 390 nm. The extinction coefficient of $H_2O_2$ (26.6 $mM^{-1}$ $cm^{-1}$) was used for the calculation.

### 4.5. Native-PAGE of SOD and amylases under differential HS

The control and HS-treated samples were used for the native-PAGE assay of SOD following the method as mentioned by Beauchamp and Fridovich [27]. In brief, 20 μg of protein from each treatment was loaded for run in 10% native-PAGE at 4°C. The gel was incubated with NBT for 15 min in dark after run followed by washing with water. Further, the gel was incubated with riboflavin for 15 min under dark condition. The gel was illuminated with light for 10–15 min leading to the appearance of white SOD activity band in the blue background. The steps for the native-PAGE of amylase enzyme were followed as explained by Kumar et al. [20]. The alcohol soluble protein fractions (25 μg) extracted from 100 mg of developing endosperm tissue was used for the native-PAGE assay. The bands appeared on the gel was scanned using Gel Doc Easy (Bio-Rad, USA).

## 5. Analyzing the effect of HS on photosynthetic rate of wheat

The flag leaf of control and HS-treated tagged plants were used for the photosynthetic rate analysis using the infra-red gas analyzer (IRGA) (LiCor 6400, LiCor Inc., USA). The method of Busch [31] was used for analyzing the performance of the photosynthetic apparatus.

## 6. Characterizing the starch accumulation and integrity of starch granules in wheat under HS

We have used 0.5 g of flour for the fractionation in hot 80% ethanol and residue retained after washing repeatedly were used

for the estimation of starch following the method as explained in Kumar et al. [20]. The dark green color formed in the final reaction mixture after adding anthrone reagent was read at 630 nm. The glucose standard was used for the calculation of starch content.

The integrity of the starch granules of wheat under HS was assessed using the transmission electron microscopy (TEM). The mature seeds were dissected into small slices using microtome and other steps for the sample fixation, dehydration and mounting on stubs were followed as explained in earlier publication [20]. The images were visualized and captured using scanning electron microscopy (Carl Zeiss) at 25 kV.

## 7. Statistical analysis

The experiment was performed using three biological replicates from each treatment. The statistical significance of the data ($P \leq 0.05$) was analyzed using One-way ANOVA.

## 8. Results

### 8.1. Identification of putative MAPK transcripts

We identified ~23,000 differentially expressed (DE) unigenes in wheat under HS through de novo transcriptomic approach. The cured data (BioProject: PRJNA171754) were functionally annotated and further classified into different groups according to their putative functions generated by Basic Local Alignment Search Tool (BLAST) analysis. Domain based homology search showed the presence of 21 novel transcripts having close resemblance with MAPK gene reported from different plant sources (Table S1).

### 8.2. Gel-based proteomic approach

The control and HS-treated samples of HD3086 and BT-Schomburgk were used for the identification of DEPs using 2-DE. The gels were scanned and the protein spots were identified using IMP7 software (GE Healthcare) version 7.0.6. (Fig. S1). The gel image of control and HS-treated samples were superimposed over each other in order to identify the DEPs. We observed 88 DEPs in HD3086 with 22 unique protein spots, whereas 58 DEPs was observed in BT-Schomburgk with 11 unique protein spots with high resolutions (Fig. 1). Based on the relative fold expression of DEPs, we selected 20 protein spots (Table S4) from both the cultivars (10 spots each) for the identification using MALDI-TOF/MS (Fig. 2). Some of the proteins identified in HD3086 are – mitogen-activated protein kinase 2 (spot ID 28), RuBisCo (spot ID 14), oxygen evolving enhancer protein (OEEP; spot ID 52), MAP kinase (spot ID 18), etc. Similarly, protein spots identified in BT-Schomburgk using MALDI-TOF/MS are – CDPK (spot ID 8), HSP16.9 (spot ID 25), SOD (spot ID 2), RuBisCo activase (spot ID 49), OEEP (spot ID 14), etc.

### 8.3. Cloning and in-silico characterization of candidate MAPK gene

Based on the information's generated from the transcriptomic and proteomic approaches, we selected MAPK (transcript_8242; spot ID 28) and MAPK (transcript_2834; spot ID 18) for the cloning. RT-PCR showed amplification of ~1.6 Kb (transcript_8242) and ~1.3 Kb (transcript_2834), as visualized on agarose gel (0.8%). Further, the amplified products were cloned, sequenced and submitted in NCBI GenBank with accession nos. KT835664 (MAPK_8242 designated as "*MAPK*") and MK854806 (MAPK_2834 designated as "*MAPK-1*").

BLASTn sequence analysis of *MAPK* and *MAPK-1* showed maximum homology with MAPK gene reported from *Hordeum vulgare* (acc. nos. AK353742 and AK376245). Similarly, protein sequence analysis of MAPK showed maximum homology with MAPK gene reported from *Zea mays* (acc. nos. NP_001167676 and XP_015643193). MAPK showed ORF of 369 amino acids, 5′ UTR of 3 aa and 3′ UTR of 79 aa. Similarly, *MAPK-1* showed ORF of 393 amino acids, 5′ UTR of 42 aa and 3′UTR of 98 aa. Conserved domain (CD) search showed the presence of Serine/Threonine Kinase (STK) domain in both the MAPK genes which is conserved functional domain of MAPK family (Fig. 3a & b). We observed 22 phosphorylation sites in MAPK with 11 threonine beyond the threshold level (Fig. 3c). Similarly, 49 phosphorylating sites were observed in MAPK-1 with 9 serine, 5 threonine, and 5 tyrosine beyond the threshold level (Fig. 3d). Based on phylogenetic analysis, the cloned MAPK genes were grouped into 4 families designated as family-I, II, III and IV; *MAPK* and *MAPK-1* cloned in present investigation belongs to family-IV (Fig. 4a & b). Signal peptide identification showed both the MAPK proteins to be nucleus-localized.

### 8.4. Heterologous expression, purification and activity assay of recombinant MAPK protein

The coding sequence of MAPK-1 (1.1 kb) was cloned in pET28a (+) vector (EMD Biosciences) and transformed in BL-21 (DE3) strain of *E. coli*. The recombinant MAPK protein was expressed by inducing with 0.9 mM concentration of isopropyl β-D-1-thiogalactopyranoside (IPTG) which showed the maximum induction. The expressed recombinant protein was purified and loaded on to SDS-PAGE in order to check the purity along with the control (vector without candidate MAPK gene). Recombinant MAPK protein showed band of ~40.2 kDa as visualized on the gel (Fig. 5a). The maximum activity of recombinant MAPK protein (6.2 U/mg proteins) was observed in response to $T_1$ (Fig. 5b).

### 8.5. Expression of MAPK-1 at transcript and protein levels

During pollination stage, the expression of *MAPK-1* was observed maximum (8.2-fold) in response to $T_1$ in HD3086, whereas minimum expression (1.9-fold) was observed in BT-Schomburgk under $T_2$ treatment (Fig. 6a). Similar pattern of expression of *MAPK-1* was observed in HD3086 and BT-Schomburgk during grain-filling stage. A significant variation was observed in the expression of *MAPK-1* in both the *cvs*. under differential HS.

Pollination stage of HD3086 showed maximum MAPK activity (1.55 U/mg proteins) under $T_1$, and minimum under $T_2$ (0.35 U/mg proteins; Fig. 6b). Similarly, grain-filling showed maximum MAPK activity under $T_2$ treatment (3.1 U/mg proteins). BT-Schomburgk during pollination stage showed maximum MAPK activity under ambient control condition (3.9 U/mg proteins) (Fig. 6b). During grain-filling, the maximum MAPK activity was observed in response to $T_2$ (6.1 U/mg proteins).

### 8.6. Expression of differentially expressed genes (DEGs) under HS

Based on the digital fold expression, we randomly selected few DEGs, as identified through transcriptome data mining [21]. We have used the following genes for the expression analysis - heat-responsive transcription factors (*HSFA6e, WRKY*), HSPs (*HSP17, HSP26*), antioxidant enzymes (*SOD*, *POX*) and genes of starch biosynthesis pathway associated enzymes [*AGPase* (large subunit) and *SSS*]. Expression analysis of *HSP26* was observed maximum (18.1-fold) in wheat *cv*. HD3086 under $T_2$ followed by *HSP17* (16.8-fold). The expression of *WRKY* TF was observed minimum under HS, when compared with other DEGs (Fig. 7a). In case of BT-Schomburgk, the maximum expression of *HSP17* (9.2-fold) was observed in response to $T_2$ (Fig. 7b).

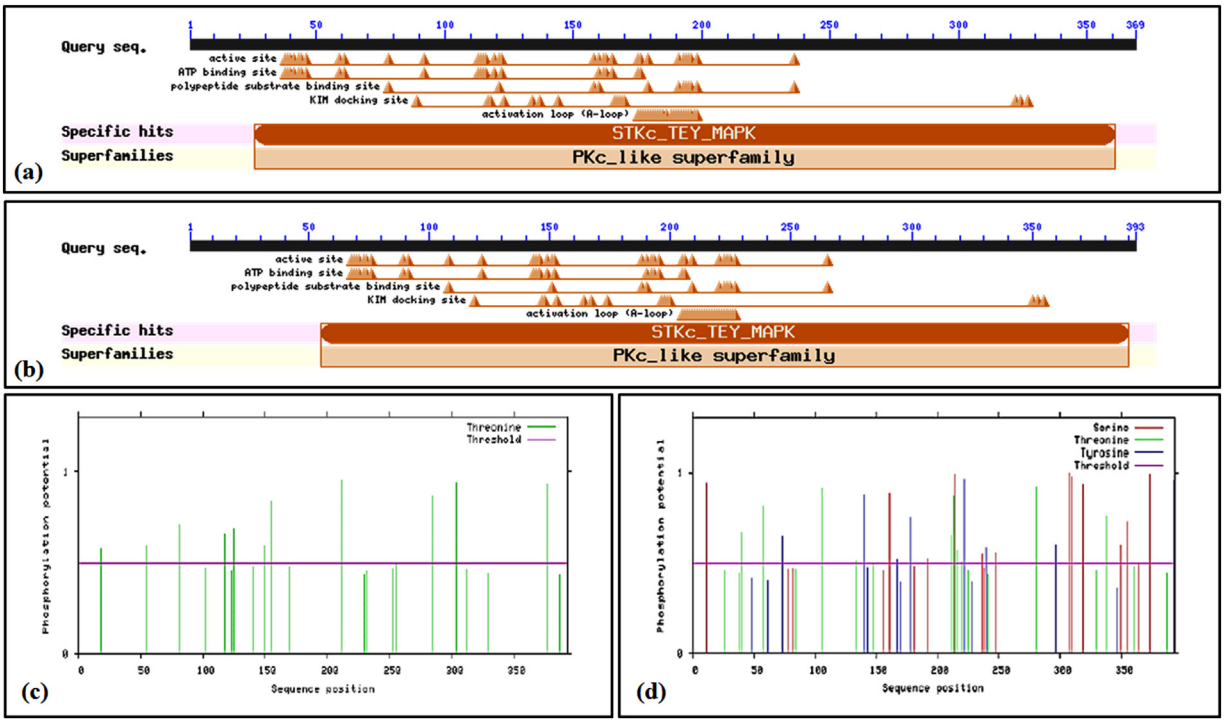


**Fig. 3.** *In silico* characterization of cloned *MAPK* and *MAPK-1* from wheat under HS; (a & b) Conserved domain analysis of MAPK and MAPK-1 genes; (c & d) Identification of phosphorylation sites in cloned MAPK and MAPK-1 genes; conserved domain search (CD) tool of NCBI (http://www.ncbi.nlm.nih.gov/Structure/cdd) was used for the domain analysis; NetPhosK was used for the identification of phosphorylation sites.

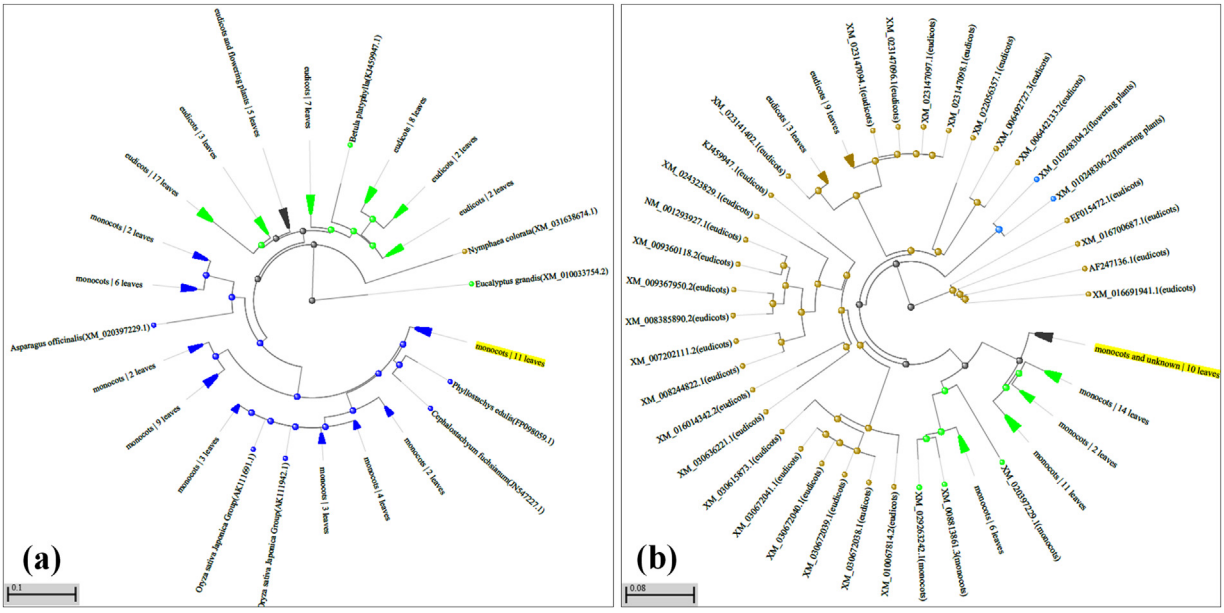


**Fig. 4.** Phylogeny trees of MAPK and MAPK-1 genes for tracing the evolutionary pattern; (a) Phylogeny tree of MAPK gene, (b) Phylogeny tree of MAPK-1 gene; the sequences of MAPK retrieved from different plant sources were used for the phylogeny analysis.

HD3086 showed maximum expression of *SOD* (3.2-fold) under $T_2$. A significant increase in the expression of *SOD* was observed with HS (Fig. 7c). Similarly, *AGPase (LSU)* and *SSS* showed maximum expression under $T_1$ and further downregulation was observed. The expression of *SSS* in HD3086 was observed maximum (1.85-fold) under $T_1$. We observed downregulation in *SSS* under $T_2$ treatment (Fig. 7c).Similarly, BT-Schomburgk showed maximum *POX* expression (3.9-fold) under $T_2$ (Fig. 7d). Abundance of *POX* transcript was observed, as compared to *SOD* under HS.

## 9. Effect of HS on traits linked with HS-tolerance

### *9.1.* In-vitro *activity of superoxide dismutase under differential HS*

Wheat *cv.* HD3086 showed maximum SOD activity (4.5 U/mg proteins) under $T_2$ during pollination stage (Fig. 8a). Similar pattern of SOD activity was observed during grain-filling stage. BT-Schomburgk during pollination stage showed maximum activity (3.5 U/mg proteins) under $T_2$ and minimum activity (2.6 U/mg

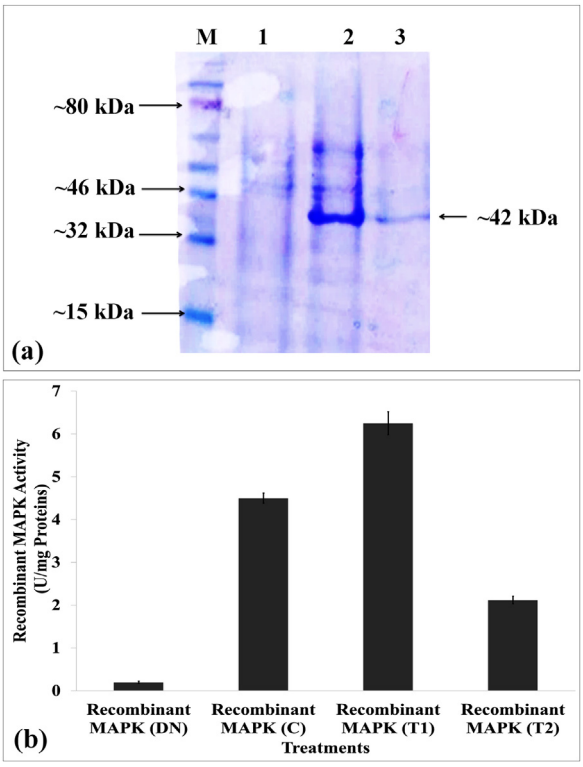


**Fig. 5.** Heterologous expression and purification of recombinant MAPK protein; (a) Visualization of recombinant MAPK protein on polyacrylamide gel electrophoresis (PAGE) gel, (b) Activity assay of purified recombinant MAPK protein under differential HS; C - 22 ± 3℃, $T_1$ - 32℃, 2 h, $T_2$ - 38℃, 2 h; denatured (DN) recombinant MAPK protein was used as negative control, vertical bars indicate *s.e* (n = 3).

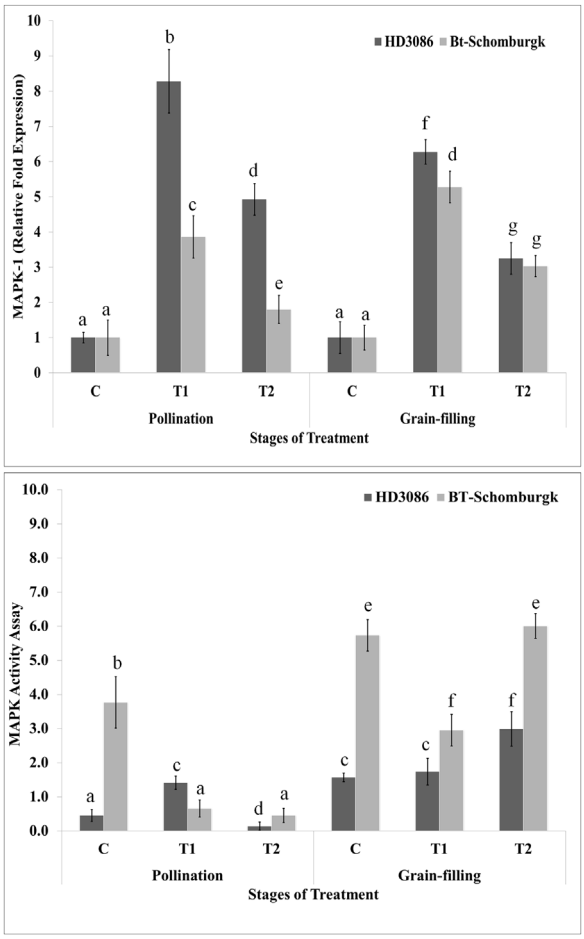


**Fig. 6.** Spatial and temporal expression and activity of *MAPK-1* and MAPK in contrasting wheat cultivars under HS at different stages of growth, (a) Expression of *MAPK-1* under differential HS, (b) Activity of MAPK under differential HS; HD3086 and BT-Schomburgk were used for the analysis; activity of the MAPK protein was carried out using ADP-Glo™ Kinase assay kit (Promega, USA), vertical bars indicate *s.e* (n = 3).

proteins) under control condition. The increase in the SOD activity was observed significant ($p \leq 0.05$) at different stages of growth and under HS.

### *9.2. Variations in the hydrogen peroxide accumulation under HS*

The accumulation of $H_2O_2$ in HD3086 (thermotolerant) during pollination stage was observed maximum (3.1 μM/g FW) under T2, whereas it was minimum during control condition (Fig. 8b). Similarly, during grain-filling stage, the $H_2O_2$ accumulation was maximum (3.8 μM/g FW) under $T_2$. Significant ($p \leq 0.05$) variations were observed in the accumulation of $H_2O_2$ at different stages of growth.

$H_2O_2$ profiling in wheat *cv*. BT-Schomburgk (thermosusceptible) during pollination stage showed maximum accumulation (2.8 μM/g FW) in response to $T_2$, whereas minimum accumulation (2.56 μM/g FW) was under control condition. Similarly, $H_2O_2$ profiling during grain-filling showed maximum accumulation (3.25 μM/g FW) under $T_2$, whereas minimum accumulation (2.95 μM/g FW) was observed under control condition. Significant variations ($p \leq 0.05$) were observed in the accumulation of $H_2O_2$ in both the contrasting wheat *cvs*. during grain-filling stage under differential HS.

#### *9.2.1. Catalase activity in wheat under differential HS*

Catalase (CAT) neutralizes the peroxide radicals inside the cells, thereby protecting the cellular organelles from damage under HS. The CAT activity in HD3086 during pollination stage was observed maximum (25.1 U $mg^{-1}$ proteins) under $T_2$ and minimum (15.3 U/mg proteins) under control condition (Fig. 8c). Similarly, during grain-filling, the maximum activity (32.1 U/mg proteins) was observed under $T_2$. We observed significant variations ($p \leq 0.05$) in the CAT activity under differential HS. CAT activity in BT-Schomburgk during pollination stage was maximum (24.1 U/mg proteins) under $T_2$ and minimum under control condition (15.2 U/mg proteins). Similarly, the CAT activity in BT-Schomburgk during grain-filling stage was observed maximum (25.1 U/mg proteins) under $T_2$ treatment; the variations in the CAT activity was observed highly significant ($p \leq 0.05$) in both the *cvs*.

### *9.3. Variations in the osmolyte accumulation under HS*

The proline accumulation in leaves of HD3086 during pollination was observed maximum (1.08 μmol $g^{-1}$ FW) under $T_2$ and minimum (0.62 μmol $g^{-1}$ FW) under control condition (Fig. 8d). During grain-filling, the accumulation was observed maximum (1.55 μmol $g^{-1}$ FW) under $T_2$, whereas minimum (0.8 μmol $g^{-1}$ FW) was observed under control condition. We observed increase in the proline accumulation in response to HS. The pattern of proline accumulation was observed similar in BT-Schomburgk under differential HS at different stages of growth. Variations in the accumulation of proline in both the *cvs*. was observed highly significant ($p \leq 0.05$) under differential HS.

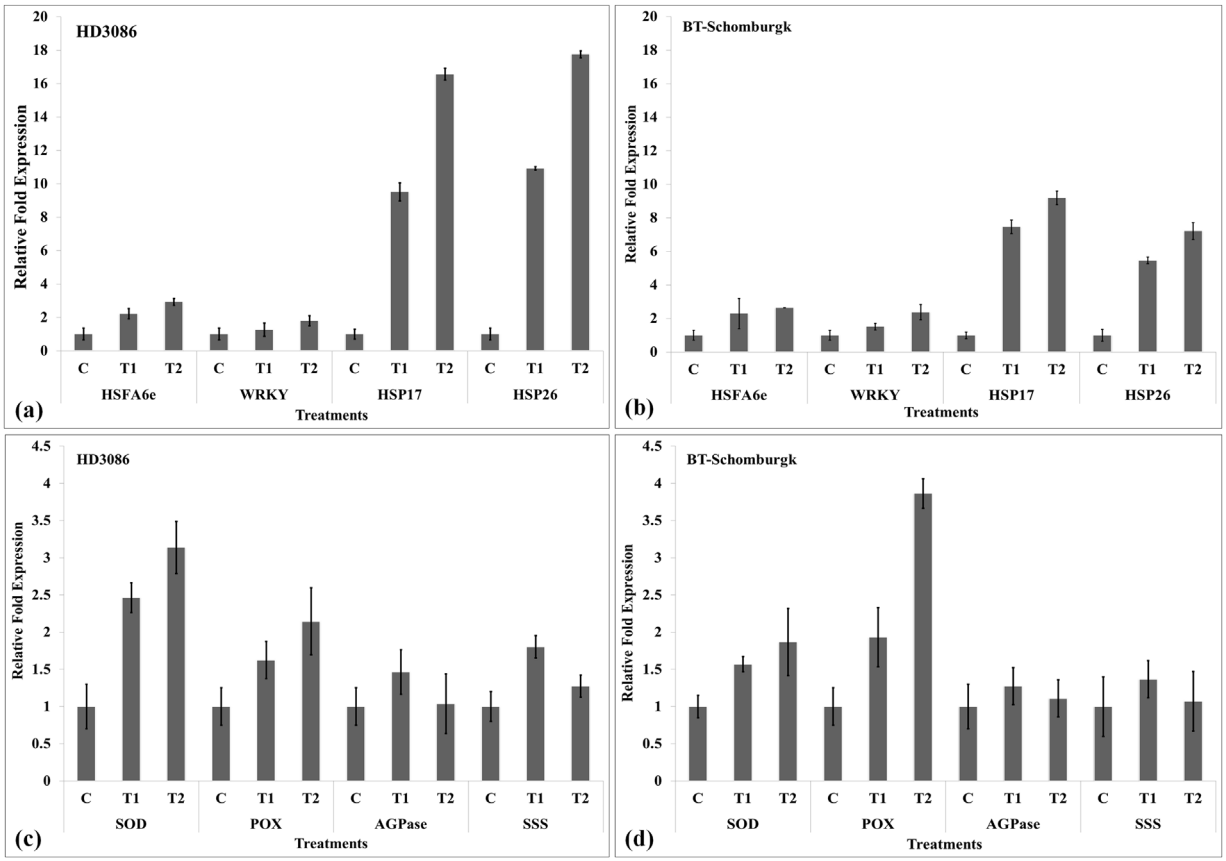


**Fig. 7.** Expression analysis of stress-associated genes (SAGs) in wheat under heat stress, (a) expression of heat-responsive TFs and HSPs in wheat *cv.* HD3086 under differential HS, (b) expression of heat-responsive TFs and HSPs in wheat *cv.* BT-Schomburgk under differential HS, (c & d) expression analysis of genes of antioxidant enzymes and starch biosynthesis pathway associated enzymes in wheat *cvs*. HD3086 and BT-Schomburgk under differential HS; TFs – *HSFA6e*, *WRKY*, HSPs – *HSP17*, *HSP26*, genes of antioxidant enzyme – *SOD*, *POX*, Genes of starch biosynthesis pathway – *AGPase (LSU)*, *SSS*; C - 22 ± 3℃, $T_1$ - 32℃, 2 h, $T_2$ - 38℃, 2 h, vertical bars indicate *s.e* (n = 3).

*9.4.* In-vivo *assay of superoxide dismutase under heat stress*

*In-vivo* activity assay of superoxide dismutase was carried out in developing endosperm and harvested seeds of wheat *cvs*. HD3086 and BT-Schomburgk under differential HS. We observed very prominent bands of manganese-SOD (Mn-SOD) and copper/ zinc-SOD (Cu/Zn SOD) in developing grains of wheat *cv.* HD3086 and faint bands of different isoforms of SODs in wheat *cv.* BT-Schomburgk under $T_1$ and $T_2$ treatments (Fig. 9a). The intensity of Cu/Zn SOD in developing grains was very high in both the *cvs*. under HS. *in vivo* assay of SOD in harvested seeds showed very prominent bands of Fe-SOD and Cu/Zn SOD, and faint band of Mn-SOD in both the *cvs*. under HS (Fig. 9b). The intensity of the bands was better in HD3086 compared with BT-Schomburgk under HS.

## 10. Characterizing the traits linked with carbon assimilation under heat stress

*10.1. Variations in the photosynthetic rate (Pn)*

The photosynthetic rate ($P_n$) of fully expanded flag leaf of control and HS-treated wheat plants were analyzed using Infra-Red Gas Analyser (IRGA). Wheat *cv.* HD3086 showed maximum photosynthetic rate (13.5 μmol $CO_2$ $m^{-2}$ $s^{-1}$) under control condition (22 ± 3 °C) during pollination stage (Fig. 10a). Photosynthetic rate was observed significantly reduced under HS; the minimum photosynthetic rate (9.03 μmol $CO_2$ $m^{-2}$ $s^{-1}$) was observed under $T_2$ (38 °C for 2 h) during grain-filling stage. Photosynthetic rate in wheat *cv.* BT-Schomburgk showed maximum $P_n$ (12.83 μmol $CO_2$ $m^{-2}s^{-1}$) under control condition (22 ± 3 °C) and minimum (9.6 μmol $CO_2$ $m^{-2}$ $s^{-1}$) in response to $T_2$ during grain-filling stage. To conclude, HS have severe effect on the photosynthetic rate of leaves in both the *cvs*.; the effect was observed more pronounced in thermosusceptible *cv.* BT-Schomburgk.

*10.2. Variations in the grain starch accumulation under HS*

Heat stress treated developing endosperm of HD3086 showed 7.9% decreases in starch compared with control (Fig. 10b). Similarly, grains of HD3086 showed 2.6% decrease in the starch under HS. Wheat *cv.* BT-Schomburgk showed 5.4% decrease in the starch content in developing endosperm in response to HS compared with control. Similarly, harvested grains exposed to HS showed 10% reduction in starch. A significant reduction ($p \leq 0.05$) in the starch content was observed in both the *cvs*., though accumulation was more stable in HD3086 (thermotolerant) compared with BT-Schomburgk.

## 11. Quality and integrity of grain starch under HS

*11.1. Variations in the structure of starch granule*

The developing grains of HD3086 and BT-Schomburgk were subjected to electron microscopy (EM) for analyzing the quality and integrity of starch granules synthesized under control (22 ± 3 °C) and HS-treated (38 °C for 2 h) conditions. We observed very bold, globular and structured starch granules with large size in case

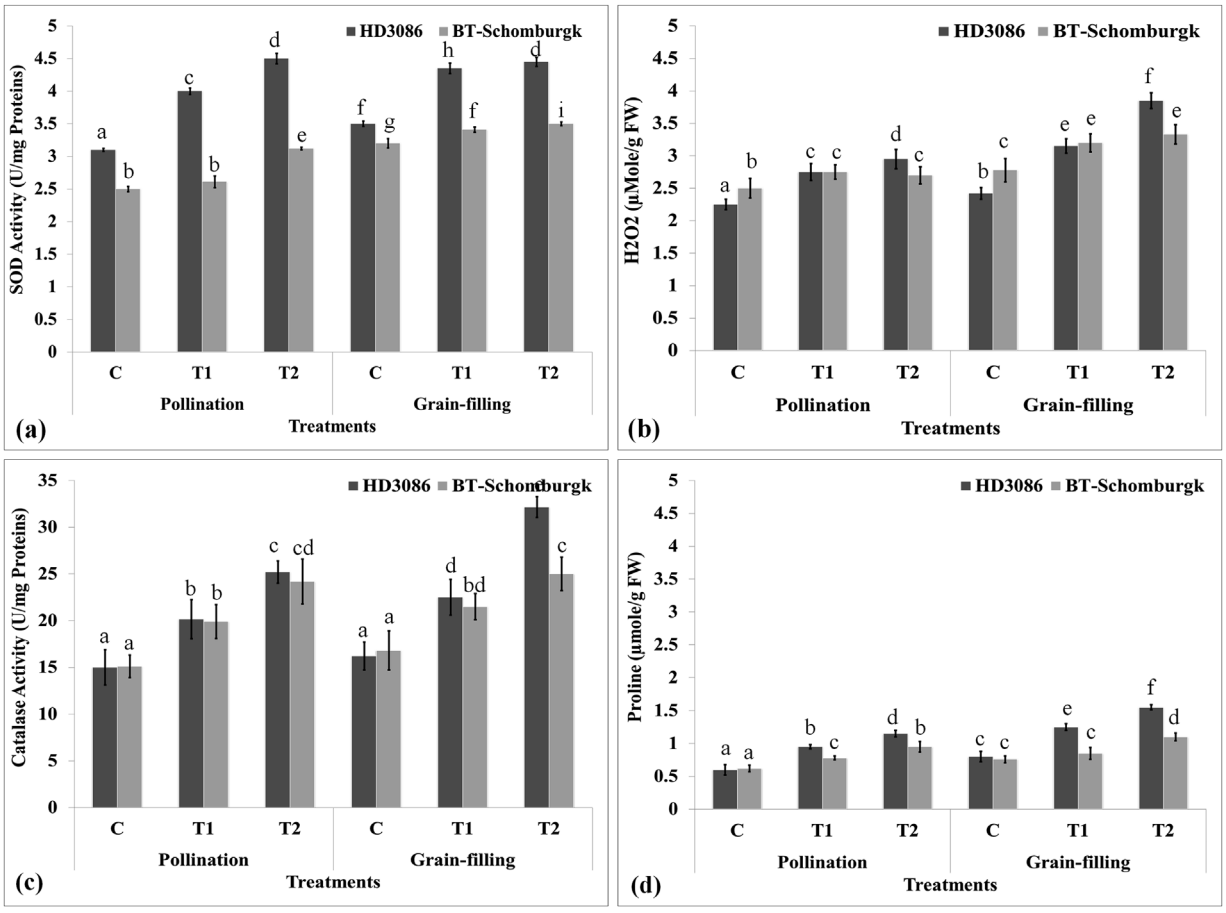


**Fig. 8.** Characterizing the thermotolerance linked biochemical markers in contrasting wheat *cvs*. exposed to differential HS at different stages of growth, (a) variations in the SOD activity in wheat *cvs*. HD3086 and BT-Schomburgk in response to differential HS, (b) accumulation pattern of hydrogen peroxide ($H_2O_2$) in wheat *cvs*. HD3086 and BT-Schomburgk in response to differential HS, (c) catalase activity assay in wheat *cvs*. HD3086 and BT-Schomburgk in response to differential HS, (d) accumulation of osmolyte in wheat *cvs*. HD3086 and BT-Schomburgk in response to differential HS; C - 22 ± 3°C, $T_1$ - 32°C, 2 h, $T_2$ - 38°C, 2 h; three biological and technical replicates were used for the expression analysis, vertical bars indicate *s.e* (n = 3).

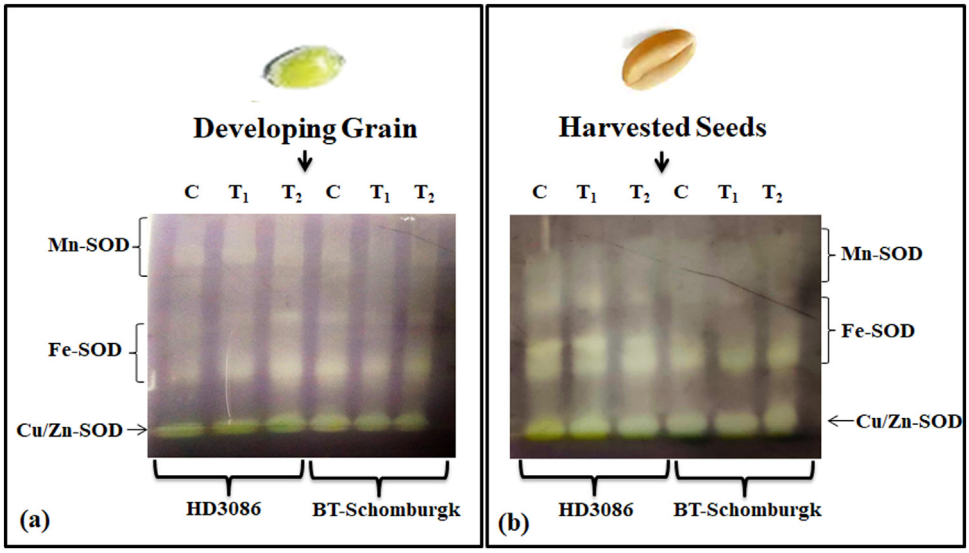


**Fig. 9.** Native-PAGE of superoxide dismutase (SOD) in developing grains and harvested seeds of contrasting wheat *cvs*. under differential HS, (a) *In-gel* activity assay of SOD in developing grains of wheat *cvs*. HD3086 and BT-Schomburgk under differential HS, (b) *In-gel* activity assay of SOD in harvested seeds of wheat *cvs*. HD3086 and BT-Schomburgk under differential HS; C - 22 ± 3°C, $T_1$ - 32°C, 2 h, $T_2$ - 38°C, 2 h; Native Gel (7%) was used for the native-PAGE.

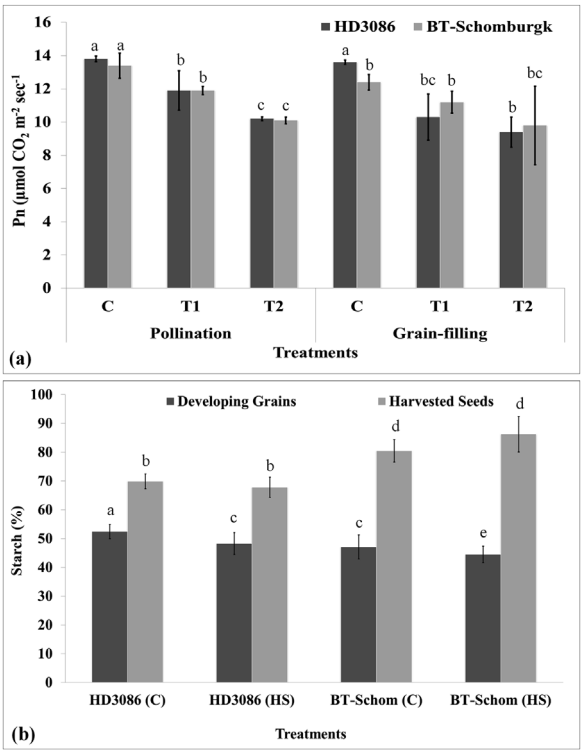


**Fig. 10.** Characterizing the carbon assimilation in contrasting wheat *cvs*. under differential HS, (a) Analyzing the photosynthetic rate ($P_n$) of wheat *cvs*. HD3086 and BT-Schomburgk under differential HS, (b) percent starch accumulation in developing grains and harvested seeds of wheat *cvs*. HD3086 and BT-Schomburgk under differential HS; C - 22 ± 3°C, $T_1$ - 32°C, 2 h, $T_2$ - 38°C, 2 h; vertical bars indicate *s.e* (n = 3).

of HD3086 under control condition; whereas small granules with less numbers and empty pockets were observed in HS-treated sample (Fig. 11a & b). Wheat *cv*. BT-Schomburgk showed spherical starch granules with pleated structure under control condition, whereas very thin and flat granules with less number was observed under HS-treated condition (Fig. 11c & d). The starch granules were glued and defragmented with flat structure in HS-treated BT-Schomburgk, which compromises the integrity and quality of the granules.

*11.2.* In vitro *amylases activity in developing endosperm and harvested grains of wheat exposed to HS*

The amylolytic activity was observed maximum (3.6 U/mg proteins) in HS-treated developing endospermic tissue of HD3086; non-significant differences were observed in the amylolytic activity of grains harvested from plants grown under control and HS-treated conditions (Fig. 12a). The amylolytic activity in BT-Schomburgk was observed maximum (3.9 U/mg proteins) in HS-treated tissue of developing grains and minimum (3.0 U/mg proteins) in harvested grains under control condition. Heat stress was observed to induce the activity of amylase in the developing endosperm and harvested grains of both the cultivars.

*11.2.1.* In vivo *amylases activity in developing endosperm and harvested grains of wheat*

The developing grains of HD3086 showed prominent isoforms of amylases under HS. Though, minimum variations in the intensity of the bands were observed under HS (Fig. 12b). BT-Schomburgk showed gradual appearance of multiple bands of amylases under differential HS treatments. The intensity of band was observed maximum in response to $T_2$. The intensity of bands in harvested seeds showed maximum amylases activity in HD3086, as compared to BT-Schomburgk under HS (Fig. 12c). The appearance and number of bands in response to treatment was observed more or less same in both the *cvs*. under the HS treatments.

## 12. Correlation of MAPK with traits linked with oxidative stress tolerance, carbon assimilation and grain-quality

The findings in present investigation were analyzed for understanding the correlation between the expression of *MAPK* and other physiochemical traits linked with tolerance, carbon flux and grain-quality of wheat under HS (Fig. S2). SOD and HSP17 is considered as potential markers for analyzing the oxidative stress tolerance level of wheat. We observed positive correlation ($R^2$ = 0.66, 0.76) between the expression of *MAPK* and activity of SOD at different stages of growth in HD3086 under HS. We established similar correlation in susceptible wheat *cv*. BT-Schomburgk at different growth stages. Similarly, positive correlation ($R^2$ = 0.58 and 0.50) was observed between the expression of *MAPK* and *HSP17* under HS. In case of BT-Schomburgk, the correlation coefficient between expression of *MAPK* and *HSP17* was 0.77 (during pollination) and 0.72 (during grain-filling) in response to HS. Similarly, photosynthetic rate represents the pace of carbon assimilation in plants. MAPK and photosynthetic rate ($P_n$) showed negative correlation in both the *cvs*. under HS. Grain quality is mainly represented in terms of size and integrity of starch and amylolytic activity determines the integrity of the starch in the grains. We observed positive correlation ($R^2$ = 0.73 and 0.82) between MAPK and amylolytic activity in developing grains of HD3086 and BT-Schomburgk in response to HS (Fig. S1). To conclude, MAPK has positive correlation with stress-associated genes (like SOD, CAT, and HSP17), amylolytic activity, and negative correlation with photosynthetic rate ($P_n$) in wheat under terminal heat stress.

## 13. Discussion

Abiotic and biotic stresses are detrimental for the plant growth and yield under open field condition [32]. Plants have inherited defence mechanisms to counter the vagaries of the nature by triggering the network of signaling molecules, antioxidant enzymes and by increasing the expression of SAGs/ SAPs [20]. Signaling molecules played very important role in making the plant robust enough to tolerate the cues of environmental factor. The sensing ability of different kinases acts as first line of defence and triggers the defense network linked with tolerance in plant system [33]. The signal transduction based on protein phosphorylation plays very important role under various extracellular stimuli in plant system [34].

MAPK cascade modulate the signaling network operating inside the plant system under various stresses [35]. MAPK acts as master regulator to maintain the various physiological and biochemical activities inside the cell in response to stresses [36]. Complex MAPK cascades are evolutionarily conserved among eukaryotic organisms [37]. MAPK is involved in diverse cellular processes such as cell growth, differentiation, and various stress responses [35]. Here, we identified 24 MAPKs in wheat and cloned two putative MAPK genes of 1.6 kb and 1.3 kb from wheat *cv*. HD3086 under HS. Few of the heat responsive *MAPK* is reported in wheat ([38]; [39] [40];). We observed the presence of Serine/Threonine Kinase (STK) in the active domain of both the MAPK genes which is conserved functional domain of MAPK family [41]. Though, MAPK-encoding genes have been also characterized in other crops like *Arabidopsis*, alfalfa, pea, wheat, rice [*OsMSRMK2*, *OsBWMK1*, *DSM1* (MAPKKK),

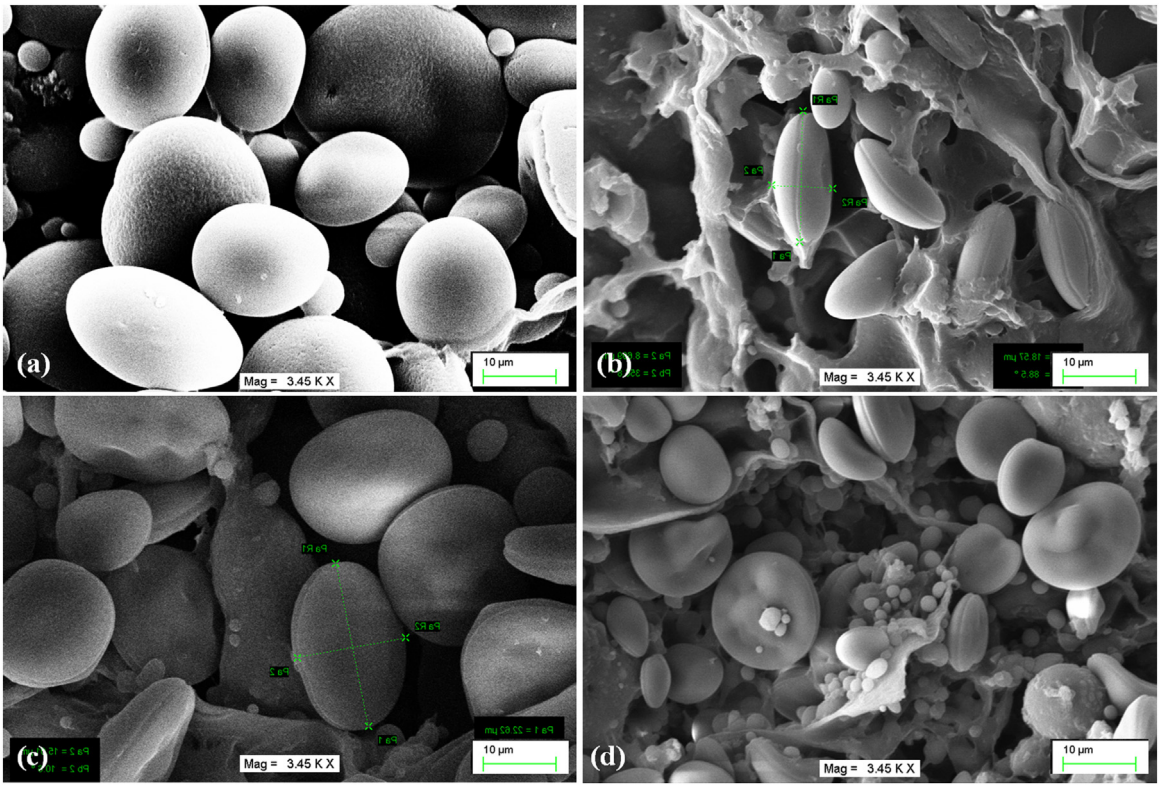


**Fig. 11.** Characterizing the ultra-structure of starch granules in contrasting wheat cultivars under HS, (a) structure of starch granule in HD3086 under control condition, (b) structure of starch granule in HD3086 under HS-treated condition, (c) structure of starch granule in BT-Schomburgk under control condition, (b) structure of starch granule in BT-Schomburgk under HS-treated condition.

*OsMPK3, OsMPK4, OsMKK4*, *MAPKK4, MAPKK1*, and *MAPKK10, OsMAPK5*], sunflower, etc. [37,42,43].

We also isolated recombinant MAPK protein of ~40.3 kDa from *E. coli* through heterologous expression. Recombinant MAPK protein showed maximum activity under $T_1$ treatment, which further decreases with increase in the temperature. *in vivo* activity of MAPK under HS showed very high activity in BT-Schomburgk (thermosusceptible) during grain-filling compared with HD3086 (thermotolerant). Pollination, being the critical stage, is more prone to elevation in temperature, as compared to grain-filling. Heat stress during pollination directly affects the pollen interaction with stigma, tube growth, fertilization and disrupts the transportation of photosynthates and accumulation in grains causing the formation of empty pockets in seeds [5]. The MAPK in case of BT-Schomburgk showed drastic reduction in the activity under $T_1$ at pollination stage. This leads to maximum yield penalty in BT-Schomburgk and is the reason behind its thermosusceptible nature, as compared to HD3086 (thermotolerant), which shows stable MAPK activity during critical stages under HS. Few researchers have reported improved stress tolerance in Arabidopsis, tobacco and cereals through genetic manipulation of MAPK [44]. Link et al. [45] reported abrupt activation of a 50 kDa MAPK in leaves of mature tomato plants under HS.

The thermotolerant wheat *cv.* HD3086 showed higher expression level of *MAPK-1* with lower activity under differential HS. The MAPK mRNA translation has tight regulation and regulates the expression of MAPK gene in response to intracellular and extracellular environmental cues [46]. Different signaling pathways interrupt the mRNA translation by inducing different inhibitors for downregulating translational machinery. Many literatures have reported that MAPK itself regulates the proteome homeostasis in order to trigger adaptive responses under stresses [47]. This may be the reason behind the higher expression level of

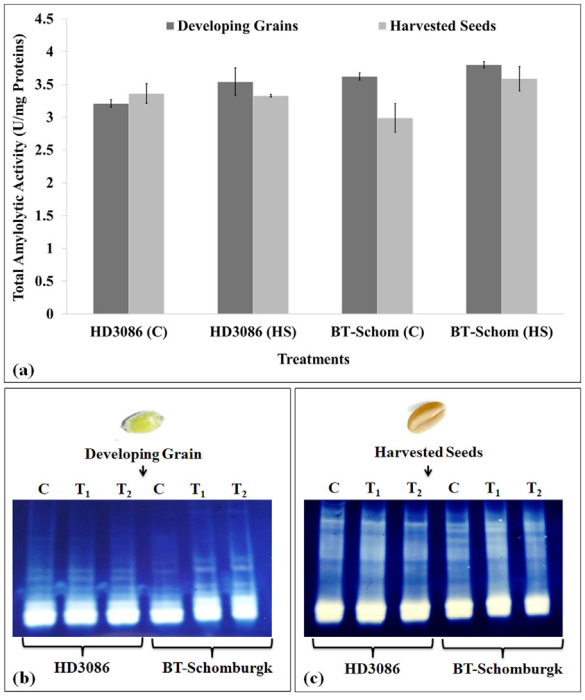


**Fig. 12.** Charactering the effect of heat stress on quality of starch in terms of amylolytic activity in developing grains and harvested seeds of contrasting wheat cultivars, (a) total amylolytic activity in developing grains and harvested seeds of wheat *cvs*. HD3086 and BT-Schomburgk under HS, (b) *In-gel* activity assay for analyzing the isoenzymes of amylases in developing grains of wheat *cvs*. HD3086 and BT-Schomburgk under HS, (c) *In-gel* activity assay for analysing the isoenzymes of amylases in harvested seeds of wheat *cvs*. HD3086 and BT-Schomburgk under HS; C - 22 ± 3°C, HS - 38°C, 2 h; vertical bars indicate *s.e* (n = 3).

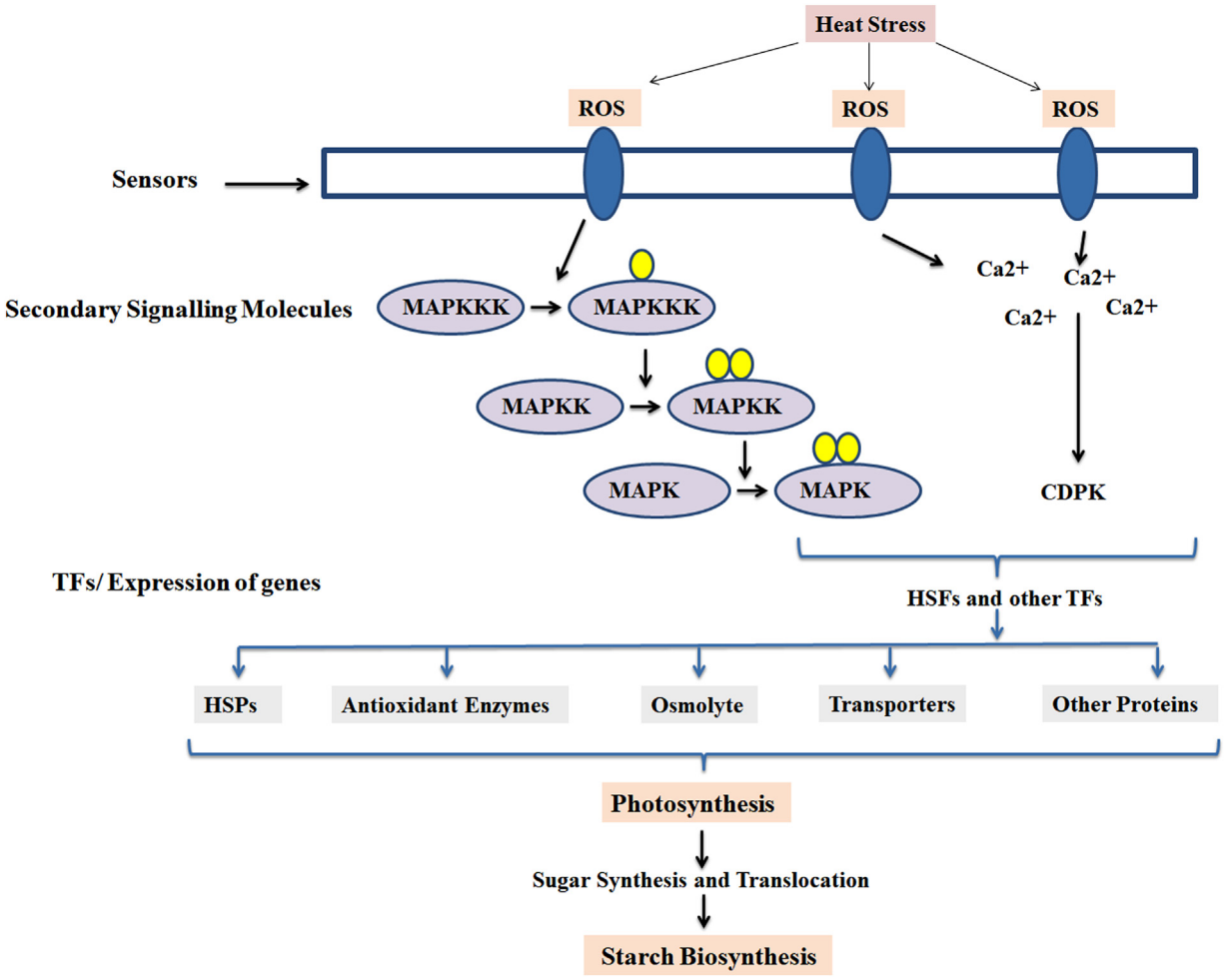


**Fig. 13.** Model hypothesizing the role of MAPK as sensors and signaling molecule in modulating the thermotolerance and carbon assimilation of wheat under HS; ROS, Reactive oxygen species; CDPK, Calcium dependent protein kinase.

*MAPK-1* with lower protein activity and it varies with the genotypes and other environmental cues.

The significant high activity of MAPK under HS was correlated with the traits linked with thermotolerance of wheat. With increase in the MAPK activity, we observed very high activity of antioxidant enzymes in HD3086 and BT-Schomburgk in response to HS. Wheat showed significant increase in the ROS and osmolyte under terminal HS. The accumulation was more significant in thermotolerant *cv.* compared with thermosusceptible *cv.* ROS and other free radicals have been reported to activate the expression and activity of MAPKs, which in turn regulate the expression of key genes linked with oxidative stress tolerance, carbon assimilation and grain-quality [48].

MAPK expression and activity was observed to have positive correlation with traits linked with tolerance, carbon flux and negatively correlated with photosynthetic rate ($P_n$) in wheat under HS. The rate of photosynthesis decreases under HS and the effect was observed more severe in thermosusceptible *cv.* compared with thermotolerant which is in conformity with the findings of Slattery and Ort [49].

The expression of SAGs like TFs (*HSF6a*, *WRKY*), HSPs (*HSP17* and *HSP26*), and antioxidant enzymes (*SOD*, *POX*) was observed maximum in thermotolerant *cv.* (HD3086) having high MAPK expression at transcript and protein level compared with thermosusceptible (BT-Schomburgk). MAPK cascade has been reported to regulate different biological process inside the plant system through signal transduction pathways [48,50]. Hydrogen peroxide, being one of the important ROS, is involved in signaling against stresses and concentration above certain limit leads to sudden death of the cells [21]. The accumulation of $H_2O_2$ was higher in HD3086 with maximum MAPK expression and activity in response to HS compared with BT-Schomburgk at different stages. $H_2O_2$ has been reported to activate different MAPKs in response to change in environmental conditions especially in maize [51] and pea [52]. MAPK has also been reported to alleviate the oxidative damage caused due to abiotic stresses [53].

Catalase neutralizes the $H_2O_2$ produced by SOD and other metabolic pathway associated reactions in crop plants. Here, CAT activity was higher in HD3086 under HS during grain-filling stage. MAPK influences the ROS level by affecting the catalase activity in plant under HS. Similar findings have been reported by Sinha et al. [7]. The accumulation of osmolyte is one of the important defence mechanisms of plants under multiple stresses. The accumulation of proline showed significant increase under HS. Qaseem et al. [54] reported similar findings in wheat. Osmotic stress activates the MAPKs as reported in *Medicago* and Tobacco [55]. MAPK-based signaling under stress condition activates the proline biosynthetic enzyme (P5CS and P5CR) and induces higher accumulation of proline [56].

According to recent report of FAO, climate change has depleted the essential nutrients from the grains. The integrity of most of the primary metabolites is compromised due to heat stress. We also observed sudden increase in the activity of macromolecule degrading enzymes especially amylases in wheat grains. The

elevation in environmental temperature increases the activity of amylases in grains which has adverse effect on grain-quality. MAPK and amylases showed positive correlation in developing grains under HS. The intensity of the stress enhances the expression and activities of MAPK and amylases in crop plants [57].

## 14. Model for hypothesizing the role of MAPK in thermotolerance

The production of ROS in response to HS triggers the expression and activity of phosphoproteins like CDPKs and MAPK cascade in crop plants. MAPK, being at pivotal position trigger the expression of TFs and other defence-linked genes like HSPs, antioxidant enzyme, osmolyte and pathway-linked genes inside the cell (Fig. 13). HSPs play dual role of protein folding and protection of nascent proteins. HS causes abrupt increase in the accumulation of $H_2O_2$ inside the cells [60]. Antioxidant enzymes protect the cell organelles from the free radicals by scavenging the ROS. MAPK indirectly regulates the defence related genes/ proteins involved in carbon assimilatory pathways under terminal HS [59]. The sugar synthesis and translocation is hampered due to HS, though SAPs actively works to protect the translocation and accumulation of photosynthates in the form of starch granules inside the endospermic tissue. Tissues having high MAPK activity showed maximum activities of HSPs and antioxidant enzymes along with the accumulation of osmolyte and antioxidants. This makes us to conclude that the activity of starch degrading enzymes is indirectly regulated by MAPK which is evident from the high quality starch granules in plants having maximum expression of *MAPK*. Even the isoform of SOD and amylases has been reported to increase in samples having high expression and activity of MAPK under HS. MAPK has been predicted to act as master switch for triggering different genes/ enzymes involved in tolerance and carbon assimilation in wheat under terminal HS without affecting the grain-quality [18].

## 15. Conclusions

To conclude, terminal HS drastically reduces the yield and grain-quality of wheat. Plants has inherited network of signaling cascade in order to protect itself from the biotic and abiotic stresses. MAPK signaling cascade regulate the tolerance and other biological mechanisms. We identified 21 novel transcripts of MAPK and cloned two putative heat-responsive MAPK genes of 1.3 kb (*MAPK*) and 1.6 kb (*MAPK-1*) from wheat under HS. A recombinant MAPK protein of ~40.3 kDa was purified, isolated and characterized to have very high *in vitro* kinase activity under HS. The expression of *MAPK* was observed maximum in HD3086 with lower protein kinases activity under HS; reason being the inhibition and tight regulation of translational processes. Expression and activity of MAPK was observed to have positive correlation with biochemical traits linked with thermotolerance and negative correlation with traits linked with carbon flux. Developing grains showed very high amylolytic activity predicted to be regulated by MAPK under HS, which indirectly affect the starch quality. The heat-induced MAPK can be used as potential thermo-sensor for analyzing the stress level of the plant. MAPK can be recommended as molecular marker for evaluating diverse germplasm of wheat for HS-tolerance. We can also use this gene to manipulate the stress signaling cascade in plants having amplified impact on over-all tolerance level - a targeted kinase based approach to develop heat tolerant wheat.

## Funding

This work was supported by the Council of Scientific and Industrial Research (CSIR) under Extra Mural Grant [grant no 38 (1436)/17/EMR-II] and Indian Council of Agricultural Research (ICAR) under National Initiative on Climate Resilient Agriculture (sanction no 12/115, TG3079).

## Declaration of Competing Interest

The authors declare that they have no known competing financial interests or personal relationships that could have appeared to influence the work reported in this paper.

## Acknowledgments

We are highly thankful to the scientists of ICAR- Indian Agricultural Statistics Research Institute for executing the bioinformatics characterization of MAPK under the CABin scheme of Indian Council of Agricultural Research (Sanction no 21-56 TG 3064).

## Appendix A. Supplementary data

Supplementary material related to this article can be found, in the online version, at doi:https://doi.org/10.1016/j.btre.2021.e00597.

## References

[1] M. Modarresi, V. Mohammadi, A. Zali, M. Mardi, Response of wheat yield and yield related traits to high temperature, Cereal Res. Commun. (2010), doi: http://dx.doi.org/10.1556/CRC.38.2010.1.3.
[2] R.R. Kumar, K. Singh, S. Ahuja, M. Tasleem, I. Singh, S. Kumar, M. Grover, D. Mishra, G.K. Rai, S. Goswami, G.P. Singh, V. Chinnusamy, A. Rai, S. Praveen, Quantitative proteomic analysis reveals novel stress-associated active proteins (SAAPs) and pathways involved in modulating tolerance of wheat under terminal heat, Funct. Integr. Genomics (2018), doi:http://dx.doi.org/10.1007/s10142-018-0648-2.
[3] K. Moustafa, S. AbuQamar, M. Jarrar, A.J. Al-Rajab, J. Trémouillaux-Guiller, MAPK cascades and major abiotic stresses, Plant Cell Rep. (2014), doi:http://dx.doi.org/10.1007/s00299-014-1629-0.
[4] C.N. Jacott, S.A. Boden, Feeling the heat: developmental and molecular responses of wheat and barley to high ambient temperatures, J. Exp. Bot. (2020), doi:http://dx.doi.org/10.1093/jxb/eraa326.
[5] R.R. Kumar, S. Goswami, G.K. Rai, N. Jain, P.K. Singh, D. Mishra, et al., Protection from terminal heat stress: a trade-off between heat-responsive transcription factors (HSFs) and stress-associated genes (SAGs) under changing environment, Cereal Res. Commun. (2020) 1–8.
[6] M. Farooq, H. Bramley, J.A. Palta, K.H.M. Siddique, Heat stress in wheat during reproductive and grain-filling phases, Crit. Rev. Plant Sci. 30 (6) (2011) 491–507, doi:http://dx.doi.org/10.1080/07352689.2011.615687.
[7] A.K. Sinha, M. Jaggi, B. Raghuram, N. Tuteja, Mitogen-activated protein kinase signaling in plants under abiotic stress, Plant Signal. Behav. (2011), doi:http://dx.doi.org/10.4161/psb.6.2.14701.
[8] M. Farooq, F. Nadeem, N. Gogoi, A. Ullah, S.S. Alghamdi, H. Nayyar, K.H.M. Siddique, Heat stress in grain legumes during reproductive and grain-filling phases, Crop Pasture Sci. (2017), doi:http://dx.doi.org/10.1071/CP17012.
[9] K. Abhinandan, L. Skori, M. Stanic, N.M.N. Hickerson, M. Jamshed, M.A. Samuel, Abiotic stress signaling in wheat – an inclusive overview of hormonal interactions during abiotic stress responses in wheat, Front. Plant Sci. (2018), doi:http://dx.doi.org/10.3389/fpls.2018.00734.
[10] G. Tena, T. Asai, W.L. Chiu, J. Sheen, Plant mitogen-activated protein kinase signaling cascades, Curr. Opin. Plant Biol. (2001), doi:http://dx.doi.org/10.1016/S1369-5266(00)00191-6.
[11] M. Cargnello, P.P. Roux, Activation and function of the MAPKs and their substrates, the MAPK-Activated protein kinases, Microbiol. Mol. Biol. Rev. (2011), doi:http://dx.doi.org/10.1128/mmbr.00031-10.
[12] T. Asai, G. Tena, J. Plotnikova, M.R. Willmann, W.L. Chiu, L. Gomez-Gomez, T. Boller, F.M. Ausubel, J. Sheen, Map kinase signaling cascade in Arabidopsis innate immunity, Nature (2002), doi:http://dx.doi.org/10.1038/415977a.
[13] M. Teige, E. Scheikl, T. Eulgem, R. Dóczi, K. Ichimura, K. Shinozaki, J.L. Dangl, H. Hirt, The MKK2 pathway mediates cold and salt stress signaling in Arabidopsis, Mol. Cell (2004), doi:http://dx.doi.org/10.1016/j.molcel.2004.06.023.
[14] R. Benhamman, F. Bai, S.B. Drory, A. Loubert-Hudon, B. Ellis, D.P. Matton, The arabidopsis mitogen-activated protein kinase kinase kinase 20 (MKKK20) acts upstream of MKK3 and MPK18 in two separate signaling pathways involved in root microtubule functions, Front. Plant Sci. (2017), doi:http://dx.doi.org/10.3389/fpls.2017.01352.
[15] D.P. Wankhede, M. Misra, P. Singh, A.K. Sinha, Rice mitogen activated protein kinase kinase and mitogen activated protein kinase interaction network revealed by in-silico docking and yeast two-hybrid approaches, PLoS One 8 (2013), doi:http://dx.doi.org/10.1371/journal.pone.0065011.

[16] H. Zhan, H. Yue, X. Zhao, M. Wang, W. Song, X. Nie, Genome-wide identification and analysis of MAPK and MAPKK gene families in bread wheat (Triticum aestivum L.), Genes (Basel). (2017), doi:http://dx.doi.org/10.3390/genes8100284.
[17] J. Bigeard, H. Hirt, Nuclear signaling of plant MAPKs, Front. Plant Sci. (2018), doi:http://dx.doi.org/10.3389/fpls.2018.00469.
[18] G. Banerjee, D. Singh, A.K. Sinha, Plant cell cycle regulators: mitogen-activated protein kinase, a new regulating switch? Plant Sci. 301 (2020) 110660.
[19] B.T.D. Miller, Growth stages of wheat, Small (1999) 4p.
[20] R.R. Kumar, M. Tasleem, M. Jain, S. Ahuja, S. Goswami, S. Bakshi, S. Jambhulkar, S.D. Singh, G.P. Singh, H. Pathak, C. Viswanathan, S. Praveen, Nitric oxide triggered defense network in wheat: augmenting tolerance and grain-quality related traits under heat-induced oxidative damage, Environ. Exp. Bot. (2019), doi:http://dx.doi.org/10.1016/j.envexpbot.2018.11.016.
[21] R.R. Kumar, S.K. Sharma, S. Goswami, G.P. Singh, R. Singh, K. Singh, H. Pathak, R. D. Rai, Characterization of differentially expressed stress-associated proteins in starch granule development under heat stress in wheat (Triticum aestivum L.), Indian J. Biochem. Biophys. 50 (2013) 126–138.
[22] S. Kundu, D. Chakraborty, K. Das, A. Pal, An efficient in-gel digestion protocol for mass spectral analysis by MALDI-TOF-MS and MS/MS and its use for proteomic analysis of Vigna mungo leaves, Plant Mol. Biol. Rep. 31 (2013), doi:http://dx.doi.org/10.1007/s11105-012-0475-x.
[23] S.F. Altschul, W. Gish, W. Miller, E.W. Myers, D.J. Lipman, Basic local alignment search tool, J. Mol. Biol. 215 (1990) 403–410, doi:http://dx.doi.org/10.1016/S0022-2836(05)80360-2.
[24] M.W. Pfaffl, G.W. Horgan, L. Dempfle, Relative expression software tool (REST) for group-wise comparison and statistical analysis of relative expression results in real-time PCR, Nucleic Acids Res. 30 (2002) e36.
[25] U.K. Laemmli, Cleavage of structural proteins during the assembly of the head of bacteriophage T4, Nature (1970), doi:http://dx.doi.org/10.1038/227680a0.
[26] M.M. Bradford, A rapid and sensitive method for the quantitation of microgram quantities of protein utilizing the principle of protein-dye binding, Anal. Biochem. 72 (1976) 248–254.
[27] C. Beauchamp, I. Fridovich, Superoxide dismutase: improved assays and an assay applicable to acrylamide gels, Anal. Biochem. (1971), doi:http://dx.doi.org/10.1016/0003-2697(71)90370-8.
[28] B. Chance, A.C. Maehly, Assay of catalases and peroxidases, Methods Enzymol. (1955) 764–765, doi:http://dx.doi.org/10.1016/S0076-6879(55)02300-8.
[29] L.S. Bates, R.P. Waldren, I.D. Teare, Rapid determination of free proline for water-stress studies, Plant Soil (1973), doi:http://dx.doi.org/10.1007/BF00018060.
[30] F. Loreto, V. Velikova, Isoprene produced by leaves protects the photosynthetic apparatus against ozone damage, quenches ozone products, and reduces lipid peroxidation of cellular membranes, Plant Physiol. (2001), doi:http://dx.doi.org/10.1104/pp.010497.
[31] F.A. Busch, Photosynthetic gas exchange in land plants at the leaf level, Methods in Molecular Biology, (2018), doi:http://dx.doi.org/10.1007/978-1-4939-7786-4_2.
[32] P. Pandey, V. Irulappan, M.V. Bagavathiannan, M. Senthil-Kumar, Impact of combined abiotic and biotic stresses on plant growth and avenues for crop improvement by exploiting physio-morphological traits, Front. Plant Sci. (2017), doi:http://dx.doi.org/10.3389/fpls.2017.00537.
[33] A. Pitzschke, A. Schikora, H. Hirt, MAPK cascade signaling networks in plant defence, Curr. Opin. Plant Biol. (2009), doi:http://dx.doi.org/10.1016/j.pbi.2009.06.008.
[34] F. Ardito, M. Giuliani, D. Perrone, G. Troiano, L.Lo Muzio, The crucial role of protein phosphorylation in cell signalingand its use as targeted therapy (Review), Int. J. Mol. Med. (2017), doi:http://dx.doi.org/10.3892/ijmm.2017.3036.
[35] P. Jagodzik, M. Tajdel-Zielinska, A. Ciesla, M. Marczak, A. Ludwikow, Mitogen-activated protein kinase cascades in plant hormone signaling, Front. Plant Sci. (2018), doi:http://dx.doi.org/10.3389/fpls.2018.01387.
[36] P.J. Krysan, J. Colcombet, Cellular complexity in MAPK signaling in plants: questions and emerging tools to answer them, Front. Plant Sci. 9 (2018) 1674.
[37] M. Cristina, M. Petersen, J. Mundy, Mitogen-activated protein kinase signaling in plants, Annu. Rev. Plant Biol. (2010), doi:http://dx.doi.org/10.1146/annurev-arplant-042809-112252.
[38] V. Sangwan, B.L. Örvar, J. Beyerly, H. Hirt, S. Dhindsa Rajinder, Opposite changes in membrane fluidity mimic cold and heat stress activation of distinct plant MAP kinase pathways, Plant J. (2002), doi:http://dx.doi.org/10.1046/j.1365-313X.2002.01384.x.
[39] H.Y. Xu, C. Zhang, Z.C. Li, Z.R. Wang, X.X. Jiang, Y.F. Shi, S.N. Tian, E. Braun, Y. Mei, W.L. Qiu, S. Li, B. Wang, J. Xu, D. Navarre, D. Ren, N. Cheng, P.A. Nakata, M.A. Graham, S.A. Whitham, J.Z. Liu, The MAPK Kinase Kinase GmMEKK1 regulates cell death and defense responses, Plant Physiol. (2018), doi:http://dx.doi.org/10.1104/pp.18.00903.
[40] Y. Lee, Y.J. Kim, M.H. Kim, J.M. Kwak, MAPK cascades in guard cell signal transduction, Front. Plant Sci. (2016), doi:http://dx.doi.org/10.3389/fpls.2016.00080.
[41] T.G. Cross, D. Scheel-Toellner, N.V. Henriquez, E. Deacon, M. Salmon, J.M. Lord, Serine/threonine protein kinases and apoptosis, Exp. Cell Res. (2000), doi:http://dx.doi.org/10.1006/excr.2000.4836.
[42] S. Zhang, D.F. Klessig, MAPK cascades in plant defense signaling, Trends Plant Sci. (2001), doi:http://dx.doi.org/10.1016/S1360-1385(01)02103-3.
[43] S. Neupane, S.E. Schweitzer, A. Neupane, E.J. Andersen, A. Fennell, R. Zhou, M.P. Nepal, Identification and characterization of mitogen-activated protein kinase (MAPK) genes in sunflower (Helianthus annus L.), Plants 8 (2019), doi:http://dx.doi.org/10.3390/plants8020028.
[44] O. Šamajová, O. Plíhal, M. Al-Yousif, H. Hirt, J. Šamaj, Improvement of stress tolerance in plants by genetic manipulation of mitogen-activated protein kinases, Biotechnol. Adv. (2013), doi:http://dx.doi.org/10.1016/j.biotechadv.2011.12.002.
[45] V. Link, A.K. Sinha, P. Vashista, M.G. Hofmann, R.K. Proels, R. Ehness, T. Roitsch, A heat-activated MAP kinase in tomato: a possible regulator of the heat stress response, FEBS Lett. 531 (2002), doi:http://dx.doi.org/10.1016/S0014-5793(02)03498-1.
[46] P.P. Roux, I. Topisirovic, Regulation of mRNA translation by signaling pathways, Cold Spring Harb. Perspect. Biol. 4 (2012), doi:http://dx.doi.org/10.1101/cshperspect.a012252.
[47] H. Huang, F. Ullah, D.X. Zhou, M. Yi, Y. Zhao, Mechanisms of ROS regulation of plant development and stress responses, Front. Plant Sci. 10 (2019) 800.
[48] L. Chen, H. Sun, F. Wang, D. Yue, X. Shen, W. Sun, X. Zhang, X. Yang, Genome-wide identification of MAPK cascade genes reveals the GhMAP3K14–GhMKK11–GhMPK31 pathway is involved in the drought response in cotton, Plant Mol. Biol. (2020) 1–13.
[49] R.A. Slattery, D.R. Ort, Carbon assimilation in crops at high temperatures, Plant Cell Environ. (2019), doi:http://dx.doi.org/10.1111/pce.13572.
[50] S.V. Ramesh, R.R. Kumar, S. Praveen, Plant transcriptional regulation in modulating cross-tolerance to stress, Priming-Mediated Stress and Cross-Stress Tolerance in Crop Plants, Academic Press, 2020, pp. 231–245.
[51] J. You, Z. Chan, Ros regulation during abiotic stress responses in crop plants, Front. Plant Sci. (2015), doi:http://dx.doi.org/10.3389/fpls.2015.01092.
[52] D. Ortiz-Masia, M.A. Perez-Amador, J. Carbonell, M.J. Marcote, Diverse stress signals activate the C1 subgroup MAP kinases of Arabidopsis, FEBS Lett. 581 (2007), doi:http://dx.doi.org/10.1016/j.febslet.2007.03.075.
[53] Q. Qi, Z. Guo, Y. Liang, K. Li, H. Xu, Hydrogen sulfide alleviates oxidative damage under excess nitrate stress through MAPK/NO signaling in cucumber, Plant Physiol. Biochem. 135 (2019) 1–8.
[54] M.F. Qaseem, R. Qureshi, H. Shaheen, Effects of pre-anthesis drought, heat and their Combination on the Growth, Yield and Physiology of diverse Wheat (Triticum aestivum L.) Genotypes Varying in Sensitivity to Heat and drought stress, Sci. Rep. (2019), doi:http://dx.doi.org/10.1038/s41598-019-43477-z.
[55] C. Jonak, L. Ökrész, L. Bögre, H. Hirt, Complexity, cross talk and integration of plant MAP kinase signaling, Curr. Opin. Plant Biol. (2002), doi:http://dx.doi.org/10.1016/S1369-5266(02)00285-6.
[56] K. Dudziak, M. Zapalska, A. Börner, H. Szczerba, K. Kowalczyk, M. Nowak, Analysis of wheat gene expression related to the oxidative stress response and signal transduction under short-term osmotic stress, Sci. Rep. 9 (2019), doi:http://dx.doi.org/10.1038/s41598-019-39154-w.
[57] C.J. Bequette, S.R. Hind, S. Pulliam, R. Higgins, J.W. Stratmann, MAP kinases associate with high molecular weight multiprotein complexes, J. Exp. Bot. 69 (2018), doi:http://dx.doi.org/10.1093/jxb/erx424.
[59] M. Nadal-Ribelles, C. Solé, G. Martínez-Cebrián, F. Posas, E. de Nadal, Shaping the transcriptional landscape through MAPK signaling, Gene Expression and Control, (2019), doi:http://dx.doi.org/10.5772/intechopen.80634.
[60] R. Ranjan Kumar, Mechanism of action of hydrogen peroxide in wheat thermotolerance - interaction between antioxidant isoenzymes, proline and cell membrane, African J. Biotechnol. 11 (2012) 14368–14379, doi:http://dx.doi.org/10.5897/AJB12.2084.